A Comparative Biomonitoring Study of Trace Metals and Organic Compounds Bioaccumulation in Marine Biofilms and Caged Mussels along the French Mediterranean Coast

BARRE Abel[1], BRIAND Jean-François[1*], VACCHER Vincent[2], BRIANT Nicolas[3], BRIAND J. Marine[4], DORMOY Bruno[5], BOISSERY Pierre[6] and BOUCHOUCHA Marc[4]

1 – Université de Toulon, MAPIEM, Toulon, France

2 – LUNAM Université, Oniris, USC 1329 Laboratoire d'Etude des Résidus et Contaminants dans les Aliments (LABERCA), Nantes, France.

3 – Ifremer, CCEM Contamination Chimique des Écosystèmes Marins, F-44000 Nantes, France

4 – Ifremer, Laboratoire Environnement Ressources Provence Azur Corse (LER-PAC), CS 20330, F-83507 La Seyne Sur Mer, France

5 – Laboratoire d'Analyses de Surveillance et d'Expertise de la Marine (LASEM) – Toulon, France

6 – Agence de l'Eau Rhône Méditerranée Corse – Délégation Paca Corse, F-13001 Marseille, France

*corresponding author : briand@univ-tln.fr, Université de Toulon - CS 60584 - 83041 TOULON Cedex 9, France

Abstract

The bioaccumulation potential of contaminants in marine environments was investigated in biofilms and compared with caged mussels for a wide range of both organic and metallic contaminants across a large geographic area. Marine biofilms were sampled after three months of sub-surface immersion at 49 locations along the 1,800 km of the French Mediterranean coast. Ten chemical elements (i.e. As, Cd, Co, Cr, Cu, Hg, Mn, Ni, Pb, and Zn) and 57 organic compounds (i.e., 18 polycyclic aromatic hydrocarbons (PAHs), 8 dioxin-like and 6 non-dioxin-like polychlorinated biphenyls (PCBs) and 25 organochlorine pesticides (OCPs)) were quantified in triplicates, revealing different multi-contaminated profiles depending on sites. Most of contaminants exhibited higher concentrations in biofilms than in mussels. Moreover, a remarkable significant and positive correlation between the concentrations in both biological matrices was observed for PAHs and PCBs, and more contaminant-dependent for OCPs and metals. These results highlighted the potential of biofilms as relevant bioindicators of the marine chemical contamination.

Highlights

- Marine biofilms accumulate a wide range of trace metals and organic compounds
- Biofilms exhibit multi-contaminated profiles associated with human activities
- Biofilms accumulates PCBs and most PAHs similarly to *Mytilus galloprovincialis*

-

Abbreviations

PHE, Phenanthrene; AN, Anthracene; FA, Fluoranthene; PY, Pyrene; B(c)F, Benzo(c)fluorene; BaA, benzo(a)anthracene; CPP, cyclopenta(c,d)pyrene; CHR, Chrysene; 5-MCH, 5-Methylchrysene; BbF, Benzo(b)fluoranthene; BjF, Benzo(j)fluoranthene; BkF, Benzo(k)fluoranthene; BaP, benzo(a)pyrene; IP, Indeno(1,2,3-cd)pyrene; DbahA, Dibenz(a,h)anthracene; BghiP, Benzo(g,h,i)perylene; DbalP, Dibenzo(a,l)pyrene; DbaeP, Dibenzo(a,e)pyrene; PeCBz, Pentachlorobenzene; HCB, Hexachlorobenzene; aHCH, α-Hexachlorocyclohexane; gHCH, γ-Hexachlorocyclohexane; aESN, α-endosulfan; bESN, β-endosulfan; Hept. Cis, Heptachlor epoxide cis; Hept. Trans, Heptachlor epoxide trans; BMLR, Biofilms/Mussels Logarithmic Ratio; C, Corsica; ER, East-of-the-Rhone; WR, West-of-the-Rhone; PAHs, Polycyclic Aromatic Hydrocarbons; DL-PCBs, Dioxin-Like Polychlorobiphenyls; NDL-PCBs, Non-Dioxin-Like Polychlorobiphenyls; OCPs, Organochlorine Pesticides; TMEs, Trace Metal Elements; LOQ, Limit of quantification.

1. Introduction

Environmental pollution from organic and inorganic contaminants is a matter of concern for coastal marine ecosystems due to its ecological impacts on marine biological communities (Halpern *et al.*, 2008; Doney, 2010). Inorganic (i.e., trace metal and metalloid elements, TMEs) and organic compounds (OCs), including polycyclic aromatic hydrocarbons (PAHs), polychlorinated biphenyls (PCBs) or organochlorine pesticides (OCPs) reach marine coastal fronts through various pathways. These include direct inputs (e.g., wastewater treatment plants, surface and ground waters' pollution loads) and diffuse inputs (urban and agricultural runoff). TMEs are naturally present and ubiquitous in marine ecosystems, but their levels are significantly increased due to improper management of mining, industrial activities (including shipping), and domestic wastes. PAHs occur naturally, particularly in crude oil and as a result of volcanic eruptions or forest fires, but are released to a greater extent by anthropogenic activities involving an incomplete combustion of hydrocarbon feedstocks (Abdel-Shafy and Mansour, 2016; Patel *et al.*, 2020). In contrast, PCBs and OCPs are exclusively anthropogenic. PCBs have been used widely in various industrial applications (e.g., in heat transfer fluids in electrical capacitors and transformers, lubricants in turbines) due to their low flammability, production costs, and high chemical stability. They have entered the environment primarily through improper disposal and spills. Organochlorine pesticides, used extensively in agriculture for pest control, have neurotoxic effects on organisms by inferring with ion channels activities. Due to their persistence, wide distribution, bioconcentration and bioamplification in organisms (Brouwer *et al.*, 1999; Tudi *et al.*, 2021), and adverse effects on non-target species, OCPs were included in the Stockholm Convention on Persistent Organic Pollutants (POPs) treaty in 2004. Although their synthesis and use have been phased out and banned in France since 1987 for PCBs and between 1970 and 2010 for OCPs, they are still detected in most aquatic and terrestrial compartments due to their persistence in the environment.

Urban and industrial activities often results in the concentration of contaminants in specific locations such as harbors, bays, industrial and wastewater treatment plant outfalls, and river mouths (Alter *et al.*, 2020; Momota and Hosokawa, 2021). Consequently, monitoring programs targeting the water column, sediment and biota have been developed to assess the extent of contamination along various coastlines (Cantillo, 1998). In France, the biological integrators network (RINBIO) has been using immersed cages of *Mytilus galloprovincialis* to monitor chemical contamination of Mediterranean seawater every three years since 1996. This monitoring covers 66 sites along the 1,800 km of the French Mediterranean coastline, from Banyuls at the French-Spanish border (42°28'35.386"N, 3°7'12.083"E) to Menton at the French-Italian border (43°46'28.132"N, 7°29'51.144"E), including around the Corsica (Briand *et al.*, 2023). The Mediterranean Sea is a semi-enclosed oligotrophic basin characterised by high salinity and surface water temperatures (> 25°C) during summer, a microtidal regime, and significant anthropic pressures (Danovaro, 2003). The studied coasts belong to the Rhone-Mediterranean-Corsican watershed, divided into three ecoregions based on their distinct hydrodynamic, physical, chemical typologies, and biogeographies (Spalding *et al.*, 2007). The continental coast is divided into two distinct ecoregions separated by the Rhone river mouth (43°19'01.2"N, 4°51'54.4"E): East-of-the-Rhone (ER) and West-of-the-Rhone (WR), while Corsica (C) is defined by its insularity (Ayata *et al.*, 2018).

Although the mussel-based approach effectively monitors the temporal trends of chemical contamination (Briand *et al.*, 2023), it faces several constraints. The physiochemical characteristics of seawater, such as oligotrophy, high

temperatures and turbidity, regulate mussel growth (Seed and Suchanek, 1992; Sarà *et al.*, 1998) and thus the accumulation of contaminants in their tissues (Andral *et al.*, 2004). The risk of introducing or spreading non-indigenous invasive species or pathogens, especially in Protected Marine Areas, is also a major concern (Tan *et al.*, 2023).

Marine biofilms are complex assemblages of highly diversified microbial communities embedded in a self-produced extracellular polymeric substances (EPS) matrix that colonize all immersed substrates in marine ecosystems. This dynamic settlement process occurs naturally and leads to heterogeneous settlement of prokaryotic and eukaryotic assemblages (Dang and Lovell, 2016). These microbial communities are shaped by several parameters, including seawater and substrate's chemical and physical properties (Oberbeckmann *et al.*, 2014; Oberbeckmann, Osborn and Duhaime, 2016; Briand *et al.*, 2017; Pinto *et al.*, 2019, Catao et al., 2021) together with planktonic inoculum microbes and grazers. Despite their inherent assets sought within bioindication frameworks (e.g., sedentary lifestyle, ubiquity, straightforward and low-cost sampling procedure), marine biofilms remain widely unstudied for their potential as passive samplers of trace metals and organic pollutants compared to their freshwater counterparts (Desrosiers *et al.*, 2013; Fernandes *et al.*, 2020; Bonnineau *et al.*, 2021; Zhang *et al.*, 2022). To date, only a few studies have addressed whether marine biofilms demonstrate similar intrinsic qualities and characteristics useful for bioindication as freshwater ones, i.e., to react to short-term environmental fluctuations (Tlili *et al.*, 2008; Barral-Fraga *et al.*, 2016), to integrate contaminants correlating with their concentrations in the water column (Hobbs *et al.*, 2019) and to reflect seawater chemical quality through community structure shifts (Kriwy and Uthicke, 2011).

The objectives of this study are to evaluate at the French Mediterranean scale (i) whether and how marine biofilms accumulate target organic compounds and metal(loid)s, (ii) how heterogeneous is the spatial distribution of accumulated contaminants in biofilms, and (iii) the (dis)similarities between their accumulation in biofilms and in mussels.

2. Materials and methods

2.1. Experimental design of the SUCHIMED biomonitoring oceanographic campaign

The experiment was conducted as part of the SUCHIMED French oceanographic campaign (BOUCHOUCHA Marc, 2021, https://doi.org/10.17600/18001619) described in Briand *et al.* (2023). Among the 66 sites monitored with mussels in 2021, 50 were selected (sites characteristics are given in Supplementary Figure S1) to study marine biofilms, considering their known contrasting contamination profiles. Three 0.8 cm-thick A4 high-density polyethylene plates were immersed at each site, resulting in 150 plates being deployed beneath mussel pouches (anchoring systems are described in Supplementary Figure S2). The anchoring systems were set in place between March 17th and April 8th, 2021, by the R/V "Europe", and recovered between June 14th and July 7th, 2021, by the "Tethys II" vessel.

2.2. Experimental design and sampling

Immediately after retrieval, two areas of approximately 210cm² each of damp biofilm material were scraped off the plates for OCs and TMEs analyses. Sterile carbon steel surgical blade mounted on a scalpel handle were used for organic compounds analyses, whereas a ceramic blade knife was used for samples dedicated to metal(loid)s elements.

Samples were stored at 4°C in 50 ml wide neck clear glass bottles and 15ml Metalfree® sterile polypropylene centrifuge tubes (Labcon, USA), respectively.

2.3. Analytical methods

TMEs and OCs respective quantifications in both mussels and biofilms were performed by the same laboratories with the same instruments to restrain analytical bias and ensure adequate data comparability.

2.3.1. Trace metals method

Each sample underwent pre-treatment steps which consisted of mechanical grinding followed by lyophilization and mineralization. After this, 9 TMEs (Cr, Mn, Co, Ni, Cu, Zn, As, Cd, and Pb) were quantified by inductively coupled plasma mass spectrometry (ICP-MS, iCAP TQ Thermo) for an initial sample mass of 200 mg dw. Total Hg was quantified by atomic fluorescence (AMA-254 Altec) with a limit of quantification (LOQ) of 0.015 $mg.kgdw^{-1}$ and an initial sample mass of 100 mg dw. BCR-414 (plankton) and NIST-2976 (mussel tissue) certified reference materials were used to assess the accuracy of the analytical measurement methods. The results are expressed in µg per g of dry biofilm weight ($\mu g.gdw^{-1}$).

2.3.2 Organic compounds methods

Biofilms samples were analyzed for PAHs, PCBs and OCPs. All these analyses were carried out according to validated methods (ISO/IEC 17025:2005 standard) based on mass spectrometry and were performed at the French national reference laboratory for PCBs and PAHs for the French Ministry of Agriculture. Units used were ng per g of dry biofilm weight ($ng.gdw^{-1}$). Detailed protocols for the quantification of PAHs, PCBs and OCPs are provided in Supplementary Text S3. The list of the 57 compounds is provided in Supplementary Table S4.

2.3.3. QA/QC and reporting of results

To ensure the quality of the analysis of PCBs, PAHs and OCPs, besides the use of appropriate internal standards in each sample, labelled external standards were systematically added at the end of each analytical process in order to determine recoveries. In addition, continuous monitoring of the analytical procedure was implemented through procedural blanks. For PCBs, since the analytical contamination is fully under control, i.e., lower than the concentration levels observed in the samples and regularly monitored through control chart, blank concentration was not subtracted for this class of contaminants unlike for PAHs and OCPs. Reproducibility was assessed using quality control samples (QC) regularly characterised over several years. The QCs were as follows: a fish oil sample naturally contaminated with PCBs and a fish sample naturally contaminated with PAHs. The LOQ was set as the concentration corresponding to a signal-to-noise ratio exceeding 3 and was calculated for each molecule, in each sample tested.

2.4. Statistical analyses

All of the statistical analyses were performed using the R software (R v.4.1.1, R Core Team).

A discriminative analysis on OCs levels was performed using the following steps: the concentrations of each of the 57 compounds were averaged for replicates located at the same site, and concentrations below LOQ were substituted with null values. Next, all compounds were summed within their respective groups (PAHs, OCPs, DL and NDL-PCBs) at

each site. High and low outliers were identified as more than 1.5 times the interquartile range above or below the third and first quartiles, respectively. The trimmed means (☐) and standard deviations (σ) were calculated from the outlier-free datasets and used to discriminate the total PAHs, OCPs, DL-PCBs, and NDL-PCBs levels of the biofilms into five classes. The chosen σ-based ranking method was adapted from the ones used in previous studies (Andral *et al.*, 2004; Briand *et al.*, 2023) and consisted in five classes. defined as reference (< ☐), low (< ☐ + σ), moderate (< ☐ + 2*σ), high (< ☐ + 3*σ) and very high (> ☐ + 3*σ). Regarding TMEs, three elements (Cd, Hg and Pb) were selected and Cu was also considered because of the low reliability of the mussel matrix for this element, its high toxicity combined with its intensive use in organic farming (Pesce *et al.*, 2024) and antifouling paints (Briant *et al.*, 2022). The four target TMEs were discriminated between five classes according to the same methodology than for the organic compounds' groups.

Mussel-accumulated OCs and TMEs concentrations from the 2021 campaign were obtained from the authors of the publication dedicated to them (Briand *et al.*, 2023). The compounds and elements quantified jointly in the two environmental matrices were included for correlation analyses, i.e., all metal(loid)s, PCBs, and PAHs but 15 of the 25 OCPs (list of excluded: β- and δ- isomers of hexachlorocyclohexane, oxychlordane, α- and γ- isomers of chlordane, cis- and trans-nonachlor, ortho-para isomers of DDD and DDE, and mirex).

The correlations between biofilms and mussels for each individual compound and element were investigated using the cor function from the *stats* package with the Pearson method and by considering the LOQ as the concentrations. The matrix in which each compound or element preferentially accumulates was determined using the log10 value of the mean (on 49 sites) of the ratio of the concentration of the element or compound X in biofilms at the site i to that in mussel tissues also at the site i.

The matrices correlations between concentrations in biofilms and in mussels were determined for all OCs and TMEs. Prior to the Mantel test, all values below the LOQs were substituted with zeros and concentration matrices were transformed into Bray-Curtis dissimilarities matrices using the *vegdist* function from the *vegan* package. Group-level matrices correlations were calculated by the implemented Mantel test (Mantel, 1967; Legendre and Legendre, 1998) using Spearman's correlation with the *mantel* function from the *vegan* package in R v4.1.1. The significance of the correlation was assessed using 9999 permutations for each test and described as statistically significant if $p < 0.05$.

3. Results

At least one plate per site was recovered except at site Cassis (*st*.17), resulting in 130 out of the 150 originally immersed plates being retrieved (87%). Triplicates were retrieved for 36 sites, duplicates for 9 and one plate for 4 sites (*st*.2, 9, 10, and 13). Losses were primarily observed to the WR ecoregion (64% recovery rate), whereas 92% and 100% of the plates were recovered in the ER and C ecoregions, respectively.

3.1. PAHs, PCBs and OCPs accumulation in marine biofilms.

Analysis of 57 compounds across 130 samples resulted in 3,108 out of the 7,410 measurements (42%) below LOQs, i.e., 168 out of 1,040 (16%) for DL-PCBs, 0 out of 780 for NDL-PCBs, 502 out of 3,250 (21%) for PAHs and 3,108 out of 7,410 (75%) for OCPs. At least one contaminant was quantified at each site.

Contamination levels were mostly classified from baseline (class 0) to moderate (class 2) for PAHs and DL-PCBs (86%), for NDL-PCB (92%), and for OCPs (96%). For PAHs and PCBs, more sites were very highly contaminated (4th class) than highly contaminated (3rd class), while for OCPs only one site was in the 3rd and 4th classes.

Total PAHs concentrations ranged from 6 to 1,033 ng.gdw^{-1} with 50% of the sites below 97 ng.gdw^{-1}. The standard deviation-based statistical discrimination method identified five sites in the fourth class for PAHs (Figure 1): decreasingly *st*.27, *st*.43 (671 ng.gdw^{-1}), *st*.21 (610 ng.gdw^{-1}), *st*.40 (547 ng.gdw^{-1}) and *st*.26 (515 ng.gdw^{-1}). Conversely, the lowest concentrations were recorded at *st*.50, *st*.64 (12.6 ng.gdw^{-1}) and *st*.47 (21.8 ng.gdw^{-1}), all in Corsica. Among the 18 targeted PAHs, fluoranthene, benzo[b]fluorene, pyrene and indeno[1,2,3-c,d]pyrene contributed the most to total PAHs concentrations across all sites with mean relative share per site of 12.9±3.1%, 10.3±2.3%, 10.3±7.9% and 9.9±3.6%, respectively.

Specifically, fluoranthene accounted for 10-20% of total PAHs, except at *st*.50 (<1%), *st*.23 (7.1%), and *st*.11 (8.6%). Phenanthrene was overrepresented at northern (*st*.52) and southern (*st*.65) Corsican sites, contributing 29.7 and 39.3% to their total PAHs contents, respectively, compared to 6.4±5.8% for the remaining 47 sites. Additionally, *st*.50, noted for its high phenanthrene and low fluoranthene contents, also had the highest proportion of benzo[a]pyrene (22.9%), contrasting with an average of 8.9±3.0% at other sites.

Similar trends were observed for DL and NDL-PCBs, showing a 100-fold increase between their respective lowest and highest values at *st*.46 (0.05 ng.gdw^{-1} and 0.4 ng.gdw^{-1}) and *st*.21 (5.0 ng.gdw^{-1}, 39.9 ng.gdw^{-1}). Four sites were classified in the fourth class for both PCBs groups (*st*.18, 19, 21, and 27) while *st*.53 was categorized in the fourth DL-PCBs class and the second class for NDL-PCBs. Values below 0.4 ng.gdw^{-1} accounted for 50% of total dioxin-like congeners, with higher concentrations at *st*.18 (2.8 ng.gdw^{-1}) and *st*.19 (3.8 ng.gdw^{-1}), and lower concentrations at *st*.29 (0.10 ng.gdw^{-1}), *st*.32 and 42 (0.11 ng.gdw^{-1}). The congener 118 predominated (60.9±7.1%) across all sites, with congeners 105 and 156 accounting for 15.5±3.3% and 8.5±2.3%, respectively. The remaining 15% included congeners 123 (5.7±8.9%), 167 (5.3±2.0%), 157 (2.2±1.2%), 189 (1.3±1.2%) and 114 (0.6±0.5%). Greater dissimilarities among sites were noted for the contributions of congeners 118 and 123, from 44% at *st*.30 to 76.9% at *st*.65. The congener 123 accounted for over three-quarters of total DL-PCBs at *st*.54 (75.5%) and *st*.44 (76.8%), with all Corsican sites below 2.6%, except *st*.50 (39.0%) and surroundings (st.46, 20.8%; st.47, 25.8%).

Values below 3.4 ng.gdw^{-1} accounted for 50% of total non-dioxin-like congeners, with higher concentrations recorded at *st*.19 (20.1 ng.gdw^{-1}) and *st*.27 (13.7 ng.gdw^{-1}), and lower concentrations at *st*.32 and *st*.47 (0.6 ng.gdw^{-1}). Accumulation of non-dioxin-like compounds varied among the six targeted congeners, with PCB-153 over-represented across all sites (38.2±3.9%), followed by congeners 138 (20.2±2.2%) and 180 (16.6±4.4%). Congeners 101, 52, and 28

contributed less, with 12.4±2.7%, 7.0±3.4% and 5.6±4.2%, respectively. The latter showed higher proportions at *st*.29, *st*.39, and *st*.46 (> 15%), as did PCB-180 at *st*.37, *st*.22, and *st*.21 (26.1, 29.4 and 29.7%, respectively).

Total OCPs concentrations ranged from 0.01 to 16.2 ng.gdw^{-1}, with 50% of all sites below 2.7 ng.gdw^{-1}. *St*.40 (16.2 ng.gdw^{-1}) was classified in the fourth class and *st*.38 (6.7 ng.gdw^{-1}) in the third class. Among all OCPs, p,p'-DDE was the major contributor (28.9±25.7% on average), exceeding half of the total OCPs in five sites: *st*.22 (51.1%), *st*.38 (67.9%), *st*.35 (69.5%), *st*.32 (77.0%), and *st*.24 (90.7%). The next predominant pesticides were p,p'-DDD, γ-HCH and δ-HCH, contributing an average of 16.7±23.4, 14.9±18.1 and 12.9±13.1%, respectively. The remaining fourteen compounds together accounted for the residual 23% of OCPs content in biofilms. p,p'-DDD was the only OCP quantified at two locations (*st*.30 and 23) and over 50% at *st*.20 and *st*.18. Among hexachlorocyclohexane isomers, δ-HCH represented 55.3% at *st*.40, and was between 30% and 40% in six locations (*st*.64, 30.2%; *st*.54, 30.6%; *st*.65, 30.9%; *st*.62, 34.3%; *st*.59, 37.8%; and *st*.50, 39.4%). γ-HCH accounted for over 50% of the total OCPs at three locations (*st*.33, 50.4%; *st*.25, 51.8%; *st*.50, 53.4%)

3.2. Trace metals and metalloids accumulation in marine biofilms.

Mercury was the only element found below the LOQ in a few samples: *st*.14 (2 replicates), *st*.23 (1 replicate), *st*.37 (3 replicates), *st*.38 (1 of the 3 replicates), *st*.54 (1 of the 3 replicates), and *st*.65 (1 replicate).

Similarly to OCs, contamination levels for trace metals were mostly classified from baseline (class 0) to moderate (class 2) for Cd (94%), for Pb (92%), for Cu (90%), and for Hg (82%). More sites were very highly contaminated (4th class) than highly contaminated (3rd class) with TMEs (Figure 2).

The values for Cu ranged from 2.9 to 75.9 µg.gdw^{-1}, with 50% of values under 13.9 µg.gdw^{-1}. Three sites belonged to the fourth class, in decreasing order: *st*.02, *st*.53 (62.8 µg.gdw^{-1}) and *st*.27 (53.6 µg.gdw^{-1}). Conversely, the lowest concentration was recorded at *st*.13. Overall, the highest Cu concentrations were observed in harbors, as well as in two third-class insular sites (*st*.19, 39.4 µg.gdw^{-1}; *st*.30, 41.1 µg.gdw^{-1}).

Regarding Cd, concentrations ranged from 0.09 to 0.69 µg.gdw^{-1}, with 50% of the values under 0.21 µg.gdw^{-1}. Two sites located in the ER ecoregion belonged to the fourth class: *st*.18 and *st*.24 (0.48 µg.gdw^{-1}). Conversely, lowest concentrations were observed at *st*.13 and *st*.27 (0.09 µg.gdw^{-1}).

The Pb concentrations varied between 0.8 to 35.9 µg.gdw^{-1}, with 50% of values under 7.9 µg.gdw^{-1}. Three sites were classified in the fourth class: *st*.27, *st*.53 (23.6 µg.gdw^{-1}) and *st*.18 (22.1 µg.gdw^{-1}).

The values for Hg peaked at *st*.27 with 0.77 µg.gdw^{-1}, and 50% of stations had concentrations lower than 0.03 µg.gdw^{-1}. In the ER ecoregion, six sites belonged to the fourth class: *st*.16 (0.17 µg.gdw^{-1}), *st*.18 (0.37 µg.gdw^{-1}), *st*.19 (0.14 µg.gdw^{-1}), *st*.21 (0.24 µg.gdw^{-1}), *st*.26 (0.30 µg.gdw^{-1}) and *st*.27 (0.77 µg.gdw^{-1}). In Corsica, the *st*.53 was also in this category with 0.32 µg.gdw^{-1}.

3.3. Relationships between trace metals elements and organic compounds in biofilms and mussels

The Mantel matrices correlation test applied between the concentrations measured in marine biofilms and those in *Mytilus galloprovincialis* from Briand *et al.* (2023) resulted in very strong and significant correlations for the 18 PAHs ($r = 0.81$, $p < 0.001$, $n = 882$) and the 8 DL-PCBs ($r = 0.92$, $p < 0.001$, $n = 392$). The 6 NDL-PCBs also revealed strong and significant correlations between the two matrices ($r = 0.46$, $p < 0.05$, $n = 294$). However, OCPs showed non-significant correlations ($r = 0.17$, $p > 0.05$, $n = 735$) for the 15 compounds in common, as did metal(loid)s ($r = 0.33$, $p > 0.05$, $n = 490$) (Table 1).

Regarding PAHs, the Mantel correlation coefficients between biofilms and mussels were higher on the ER ($r = 0.80$; $n = 396$) and C (0.79; 288) ecoregions compared to the WR (0.47; 198). Conversely, a greater correlation was found for OCPs in the WR ($r = 0.21$, $p < 0.05$, $n = 165$) compared to the ER and C. Slight differences were observed for PCBs, which were still strongly correlated in each ecoregion for non-dioxin-like and dioxin-like congeners, respectively. Metal(loid)s concentrations were positively and significantly correlated on the continental coasts, i.e., WR and ER ecoregions, but not significant in Corsica.

Individually, the PAHs correlation values ranged from 0 for PY to 0.9 for IP (Figure 3). Weakly correlated PAHs included PHE ($r = 0.14$), AN ($r = 0.02$), PY, and DbalP ($r = 0.28$). Moderately correlated ones were BcF ($r = 0.57$) and 5-MCH ($r = 0.40$). The remaining PAHs showed strong correlation values above 0.7, i.e., FA ($r = 0.71$), DbaeP ($r = 0.76$), BjF ($r = 0.77$), CPP ($r = 0.78$), BaA ($r = 0.8$), BaP ($r = 0.84$), CHR and DbahA ($r = 0.84$ for both), BbF ($r = 0.87$), BkF ($r = 0.88$), BghiP ($r = 0.88$), and IP. Correlations for PCBs ranged from $r = 0.31$ (congener 123) to $r = 0.67$ (congener 167). Three congeners had correlation values < 0.5 (PCBs 123, 28, and 157). Eleven congeners had correlation values > 0.5, i.e., PCBs 52, 101, 105, 114, 118, 138, 153, 156, 167, 180, and 189. Several OCPs showed no correlation, i.e., bESN ($r = -0.3$), dieldrin and p,p'-DDT ($r = -0.08$ for both), o,p'-DDT ($r = -0.02$), HCB ($r = 0.03$), Hept. Cis ($r = 0.06$), gHCH and aESN ($r = 0.11$ for both), aHCH ($r = 0.15$), PeCBz ($r = 0.23$), Hept. Trans ($r = 0.24$) and endrin ($r = 0.29$). Heptachlor, p,p'-DDE and p,p'-DDD were moderately correlated ($r = 0.41$, 0.48 and 0.63, respectively). Regarding trace metals and metalloids, the correlation values for Zn and As were $r = -0.01$ and $r = 0.02$. Cu was weakly correlated ($r = 0.12$) as well as Cd ($r = 0.27$). Co, Cr, and Mn were moderately correlated ($r = 0.39$, 0.44 and 0.57, respectively). Ni, Pb and Hg were strongly correlated ($r = 0.61$, 0.62 and 0.84, respectively).

The differences between the accumulated concentrations in the two matrices showed that 9 out of the 57 targeted compounds and elements were more accumulated in mussels, i.e. had a negative logarithmic ratio of biofilms/mussels (BMLR) site-averaged concentrations (Figure 3). All PAHs bioaccumulate predominantly in biofilms, with a minimum BMLR of 0.85 for dibenz[a,l]pyrene and a maximum one of 2.12 for anthracene. PCBs 167, 153, 138 and 105 were slightly more accumulated in mussels, whereas the 10 other congeners were more accumulated in biofilms with a maximum BMLR of 0.97 for PCB 180. Regarding OCPs, all except p,p'-DDD were more accumulated in biofilms with a maximum BMLR of 1.32 for hexachlorobenzene. As for Trace metals and metalloids, Hg, As, Zn and Cd were more accumulated in mussels with Cd being the only targeted analyte having a BMLR < -0.5. Conversely, Mn showed the highest BMLR (1.6).

4. Discussion

4.1. Bioaccumulation of organic compounds and trace elements in marine biofilms reveals spatial heterogeneity in the contamination along the French Mediterranean coasts

Our results based on the accumulation of 57 OCs and 10 TMEs in marine biofilms after three months of immersion across 49 sites along the French Mediterranean coast unveiled significant spatial heterogeneity in both OCs and TMEs levels.

Spatial heterogeneity in the distribution of PAH, PCB, OCP and TME contamination reflects varying levels of urbanization along the coast, with major cities exhibiting higher contamination levels and a greater diversity of contaminants. This pattern aligns with previous studies highlighting urbanization and water resource usage as major contributors to chemical contamination in aquatic environments (Inglis and Kross, 2000; Dsikowitzky and Schwarzbauer, 2014). Sites with elevated contamination levels, particularly those classified in the 3rd and 4th contamination classes, were predominantly located near densely populated cities and their associated wastewater treatment plant (WWTP) outfalls. Notable multi-contamination hotspots included the breakwater of Marseilles' harbor (*st*.18), Marseilles' WWTP outfall (*st*.21), the small bay of Toulon (*st*.27), Villefranche's bay (*st*.40), and Bonifacio's harbor (*st*.52). Harbors collect a multitude of waste materials, including those generated by industrial activities (e.g., shipping, Navy) and urban sources (wastewater, runoff). This results in contamination levels that are particularly high (Tessier *et al.*, 2011; Araújo *et al.*, 2019). However, significant variability was observed within individual sites. For instance, *st*.18 and *st*.19 near Marseilles showed 4th class contamination levels for DL-PCBs (12.1 and 20.1 ng.gdw-1), but varied levels for PAHs (3rd and 2nd classes) and OCPs (baseline and 1st classes). Similarly, in the bay of Toulon, *st*.26 and *st*.27 exhibited 4th class Hg levels (0.29 and 0.77µg.gdw-1), yet differed in Cu (2nd and 4th classes), Cd (2nd and baseline) and Pb (1st and 4th) concentrations, consistent with previous findings of high Cu and Pb concentrations in Toulon biofilms (Lenoble *et al.*, 2024). Furthermore, beyond major cities, other contamination hotspots influenced by the Rhone River included *st*.15 to 17 and showed high levels of NDL-PCBs, OCPs, Hg and Cu.

Environmental parameters such as hydrodynamics, nutrient availability, and temperature or salinity are reported to shape biofilm communities and their EPS matrices, possibly influencing their contaminant interactions (Blanco *et al.*, 2018; Briand *et al.*, 2022). Diverse environmental conditions across the 1,800 km of coastline likely contributed to the variability in biofilm compositions and contaminant accumulation observed. This is supported by photographic and Scanning Electron Microscopy analyses showing different substrate colonization and biofilm compositions, provided in Supplementary Figure S5. Thus, the variability in biofilm contamination cannot be solely attributed to differences in contaminant inputs but also linked to intrinsic characteristics of the biofilms themselves. Environmental parameters such as hydrodynamics, nutrient availability, and temperature also shape biofilm communities and their EPS matrices, influencing their contaminant interactions (Blanco *et al.*, 2018; Briand *et al.*, 2022). Diverse environmental conditions across the 1,800 km of coastline likely contributed to the variability in biofilm.

Biofilm matrices play a crucial role in contaminant sorption. EPS matrices in biofilms are known to adsorb apolar organic compounds and inorganic ions due to their diverse charged and hydrophobic functional groups, derived mainly

from proteins and polysaccharides (Flemming and Wingender, 2010; Wang *et al.*, 2024). These functional groups are instrumental in accumulating chlorinated organics and their hydrolysis products (Wolfaardt *et al.*, 1994, 1998), and the uptake of various pollutants is influenced by their physical partitioning properties (Hobbs *et al.*, 2019; Zhang *et al.*, 2022). EPS matrices, especially those rich in carboxyl-containing polysaccharides, bind divalent cations effectively (Lin *et al.*, 2020). In environments where both TMEs and OCs are present, competitive and synergistic adsorption interactions can occur (Wang *et al.*, 2020).

Although it remains unclear how environmental parameters influence TMEs and OCs concentration in biofilm, the observed contamination levels globally align with historical and present environmental contexts of the sites. Measuring chemical contaminants directly in seawater over extended periods is challenging; hence, biofilms, like caged mussels (a standard bioindicator) offer valuable insights into coastal chemical contamination (Andral *et al.*, 2004).

4.2. Complementarities and specificities between biofilms and mussels' interactions with OCs and TMEs

Comparison of the chemical contamination across 49 sites in the French Mediterranean using marine mussels, a conventional bioindicator, and biofilms, an emerging technique in marine environments, revealed varying degrees of correlation.

The bioaccumulation of organic compounds is primarily influenced by their lipophilicity, persistence in the aquatic environment, and the limited ability of marine organisms to metabolize and excrete them. In contrast, the bioaccumulation of metals depends on their metabolic roles in organisms (i.e., essential vs. non-essential); most marine organisms can regulate essential metals (e.g., Cu, Zn, Mn, Fe) concentrations in their tissues as long as their environmental concentrations undershoot defined thresholds values (Kraak *et al.*, 1992), whereas non-essential ones will bioaccumulate according to ambient concentrations (Bouchoucha *et al.*, 2018).

Here, significant and high correlations values between biofilms and mussels were found for all targeted PAHs besides PHE, AN, PY and DbalP, showing that marine biofilms are suitable in quantitatively assessing PAHs-related contamination along the French Mediterranean coast including highly contaminated spots. However, poor correlations for PHE, AN, and PY can be explained by diverging accumulation pathway between mussel feeding behavior, which involves plankton consumption, and biofilms which accumulate bioavailable dissolved pollutants (Soto *et al.*, 2011). In oligotrophic environments (like in the C ecoregion), bottom-up factors (i.e., limited nutrient inputs) shrink plankton size (Derolez *et al.*, 2020); this favors fractions with significantly higher mean PAHs concentrations (Guigue *et al.*, 2023), hence leading to a possible discrepancy in PAHs accumulation between biofilms and mussels. Conversely, DbalP was below the LOQs across all sites in mussels, and therefore correlated to biofilms solely on the values of the LOQ that are sample weight-related, and whose fluctuations probably does not reflect the spatial distribution of this compound.

All DL and NDL-PCBs correlation values were significant and substantiate similar pathways of accumulation in the two matrices with biofilms-based monitoring giving close results as mussels' one. Indeed, plankton size fractions does not

differ significantly in terms of PCBs contents (Tiano *et al.*, 2014) which can harbinger consistent accumulation regardless of the trophic state.

Regarding TMEs, essential trace metals (e.g., Cu and Zn) exhibited poor correlation, likely due to the metabolic regulation of these elements by mussels (Kraak *et al.*, 1992). Considering biofilms, Richard et al. (2019) demonstrated biofilms potential in trace metals accumulation, including copper and lead. Then Djaoudi et al. (2022) reported that copper accumulation in biofilms was correlated with copper seawater concentrations. Conversely, non-essential trace metals (e.g., Hg and Pb) showed strong correlations between biofilms and mussels.

In addition to the influence of the compounds' chemical characteristics and the bioindicators' physiological traits, the Mantel correlations suggest that the spatial variability of environmental conditions also affects bioaccumulation processes in biofilms and mussels. This is indicated by lower correlation values for PAHs and NDL-PCBs and higher correlation values for DL-PCBs, OCPs, and metal(loid)s in the WR ecoregion. However, the diversity of environmental parameters that fluctuate between these ecoregions makes it difficult to interpret their individual influence on bioaccumulation, hence more studies are required to improve our understanding of these phenomena.

Moreover, the robustness of a bioindicator cannot be fully assessed through a single sampling campaign at a given time; rather, it is best evaluated by examining the variations of the bioaccumulated contaminants it exhibits over time across multiple sampling campaigns, providing a more comprehensive and reliable indication of environmental pollution changes.

5. Conclusions

To the best of our knowledge, this is the first large-scale immersion study investigating the accumulation of OCs and TMEs in marine biofilms compared with their accumulation in mussels.

As most of the contaminants appeared highly bioaccumulated in biofilms compared to mussels, together with significant positive correlations between the two biological matrices, monitoring chemical contamination using biofilms provides a comprehensive understanding of environmental contamination. This approach complements traditional mussel monitoring, allowing better assessment of certain contaminants such as Cu, technical feasibility and reliable results.

Our findings reveal that PAHs and PCBs pollution is predominantly localized around major urban areas (e.g., from *st*.16 to *st*.21, at *st*.27, and *st*.43) whereas OCPs contamination is concentrated in agricultural production zones (e.g., at *st*.11, *st*.38, and *st*.40), and trace metals are chiefly abundant in harbors, at WWTP outfalls and at river mouths. Historical legacy pollutions, such as Pb and Cu at *st*.27 and Cr and Ni at *st*.65, are also highlighted through biofilms.

Overall, marine biofilms seem to be a reliable, promising, and complementary tool to mussels in monitoring chemical contamination of these compounds and elements in marine environments, thereby contributing to more effective

environmental protection strategies. However, several steps are necessary before biofilm can be effectively integrated into chemical monitoring programs. Specifically, a deeper understanding is required of the processes and kinetics of contaminant accumulation in biofilms, as well as the precise relationships between biofilm composition and these accumulation processes.

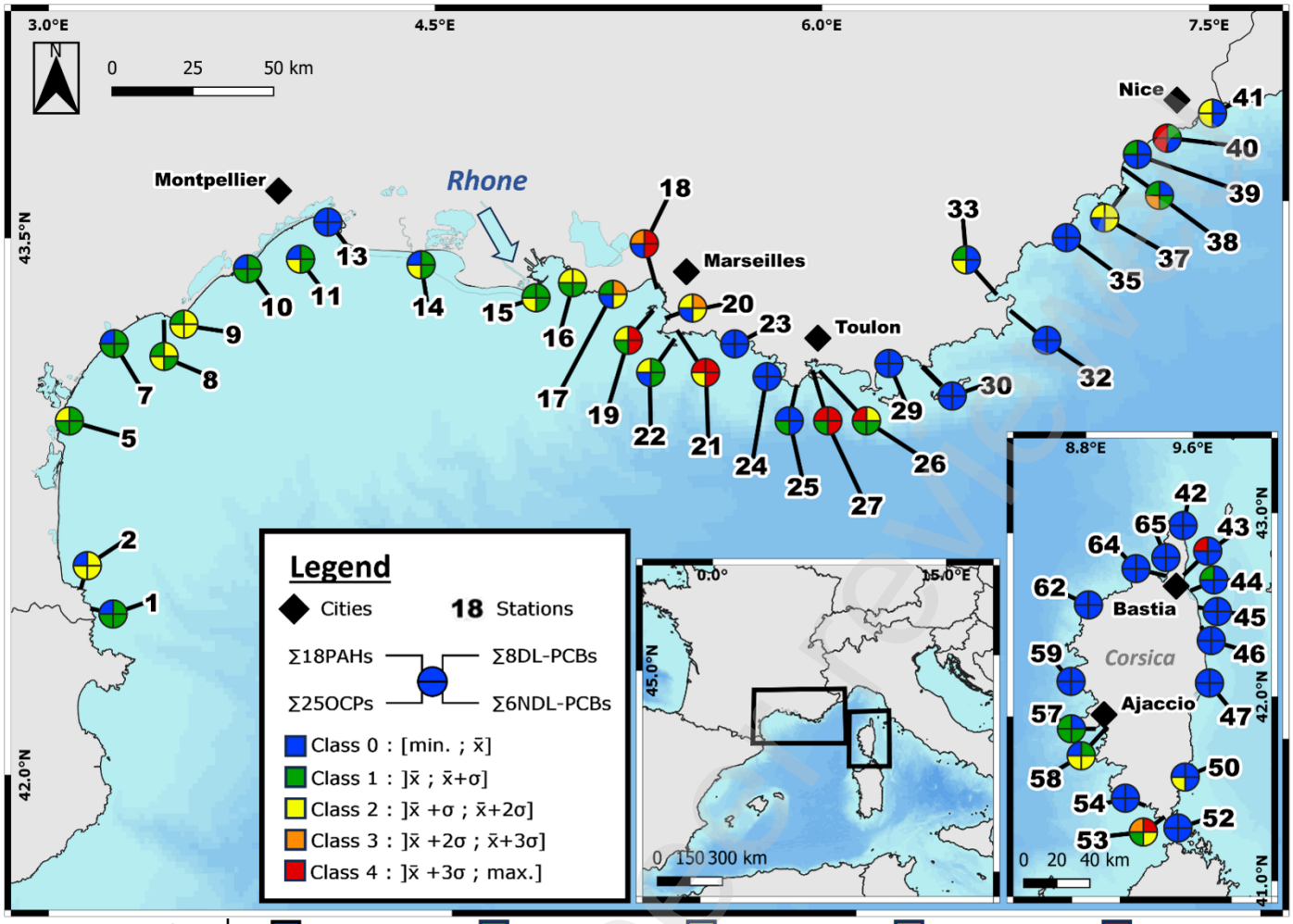

OCs (ng.gdw^{-1})	Class 0	Class 1	Class 2	Class 3	Class 4
∑18 PAHs	[6.2; 110.8]	]110.8; 196.3]	]196.3; 281.9]	]281.9; 367.4]	]367.4; 1033.2]
∑8 DL-PCBs	[0.05; 0.5]	]0.5; 0.9]	]0.9; 1.3]	]1.3; 1.7]	]1.7; 5.0]
∑6 NDL-PCBs	[0.4; 3.6]	]3.6; 6.4]	]6.4; 9.2]	]9.2; 11.9]	]11.9; 39.9]
∑25 OCPs	[0.01; 1.9]	]1.9; 2.8]	]2.8; 4.7]	]4.7; 6.7]	]6.7; 16.2]

*Figure 1 : Geographical location of the 49 sampling sites. Major cities are represented by black diamonds. Each site is represented by a pie chart divided into four quadrants symbolizing the four organic compounds families. Upper-left quarter refers to the biofilms' total PAHs concentrations. Upper-right one to DL-PCBs, lower-right one to NDL-PCBs and lower-left one to OCPs. Each quarter is coloured according to the class of contamination. Blue refers to the reference (< mean), green to low (< mean + SD), yellow to moderate (< mean + 2*SD), orange to high (<mean + 3*SD) and red to very high (> mean + 3*SD) contamination levels.*

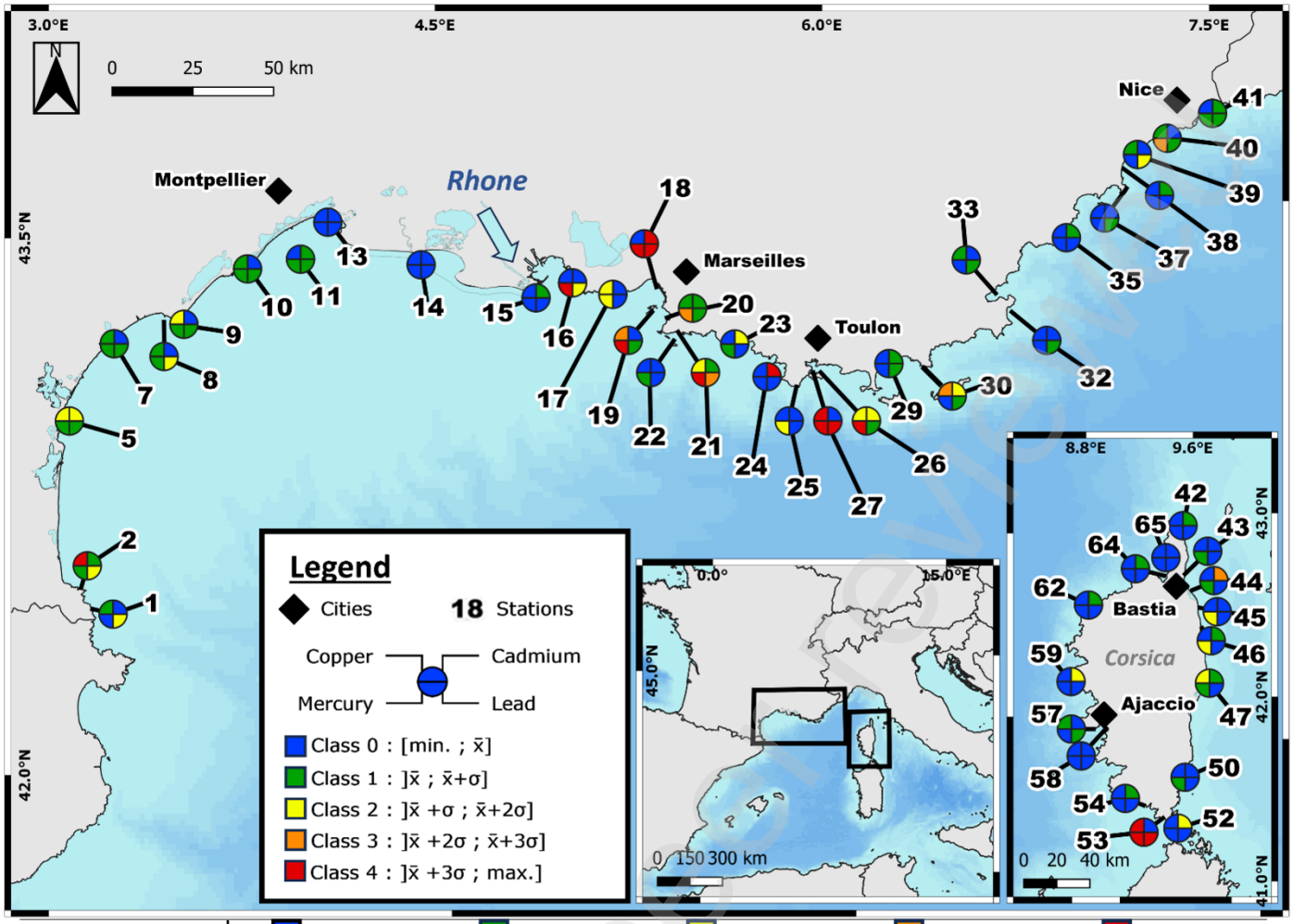

TMs (µg.gdw^{-1})	Class 0	Class 1	Class 2	Class 3	Class 4
Copper	[2.9; 19.1]	]19.1; 27.4]	]27.4; 35.7]	]35.7; 44.0]	]44.0; 75.9]
Cadmium	[0.09; 0.22]	]0.22; 0.29]	]0.29; 0.36]	]0.36; 0.44]	]0.44; 0.69]
Lead	[0.8; 7.8]	]7.8; 11.8]	]11.8; 15.8]	]15.8; 19.8]	]19.8; 35.9]
Mercury	[0; 0.03]	]0.03; 0.06]	]0.06; 0.07]	]0.07; 0.10]	]0.10; 0.77]

Figure 2 : Geographical location of the 49 sampling sites. Major cities are represented by black diamonds. Each site is represented by a pie chart divided into four quadrants symbolizing the four organic compounds families. Upper-left quarter refers to the biofilms' total PAHs concentrations. Upper-right one to DL-PCBs, lower-right one to NDL-PCBs and lower-left one to OCPs. Each quarter is coloured according to the class of contamination, the same as in Fig. 1.

*Table 1 : Mantel matrices correlation values between mussels and marine biofilms for organic compounds (PAHs, DL and NDL-PCBs, OCPs) and inorganic elements on the whole 49 sites as well as on each ecoregion (Est-Rhone, West-Rhone, and Corsica). The test significance follows Spearman's rank correlation values and is represented as follows : nothing ($p > 0.05$); * ($p < 0.05$); ** ($p < 0.01$); *** ($p < 0.001$). The number of rows/columns in each of the distance matrices is given after semicolon.*

Dataset (nb. of observations)	PAHs (18)	DL-PCBs (8)	NDL-PCBs (6)	OCPs (15)	Metal(loid)s (10)
Whole (49)	0.81***; 882	0.92***; 392	0.55*; 294	0.06*; 735	0.33; 490
West-Rhone (WR, 11)	0.47***; 198	0.98***; 88	0.41; 66	0.21*; 165	0.41*; 110
East-Rhone (ER, 22)	0.80***; 396	0.91***; 176	0.43; 132	0.09; 330	0.39*; 220
Corsica (C, 16)	0.79***; 288	0.78***; 128	0.46; 96	0.10; 240	0.26; 160

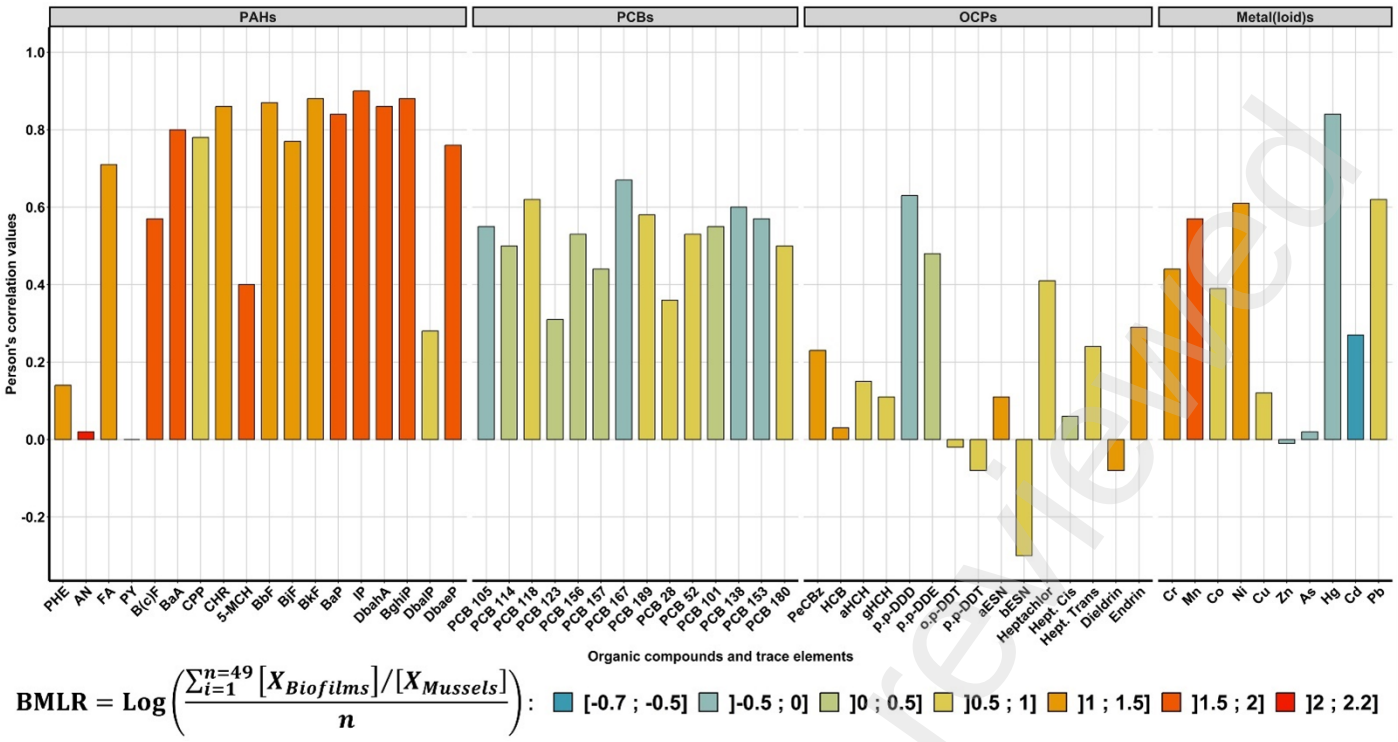

Figure 3 : Pearson's correlation values for each individual organic compound, trace metal and metalloid. The colour code indicates the matrix where a compound or element is preferably accumulated : Bluish bars show elements that are more accumulated in mussels than in biofilms, reddish ones are more accumulated in biofilms than in mussels. Abbreviations are (i) for PAHs : PHE, Phenanthrene; AN, Anthracene; FA, Fluoranthene; PY, Pyrene; B(c)F, Benzo(c)fluorene; BaA, benzo(a)anthracene; CPP, cyclopenta(c,d)pyrene; CHR, Chrysene; 5-MCH, 5-Methylchrysene; BbF, Benzo(b)fluoranthene; BjF, Benzo(j)fluoranthene; BkF, Benzo(k)fluoranthene; BaP, benzo(a)pyrene; IP, Indeno(1,2,3-cd)pyrene; DbahA, Dibenz(a,h)anthracene; BghiP, Benzo(g,h,i)perylene; DbalP, Dibenzo(a,l)pyrene; DbaeP, Dibenzo(a,e)pyrene; (ii) for OCPs : PeCBz, Pentachlorobenzene; HCB, Hexachlorobenzene; aHCH, α-Hexachlorocyclohexane; gHCH, γ-Hexachlorocyclohexane; aESN, α-endosulfan; bESN, β-endosulfan; Hept. Cis, Heptachlor epoxide cis; Hept. Trans, Heptachlor epoxide trans. All correlations were significant ($p < 0.05$, $n = 38$ for DL-PCBs 105 and 114, pentachlorobenzene, α- and β-endosulfan, $n = 39$ for DL-PCBs 123, 156, 157, 167 and 189, and $n = 49$ for all the other elements and compounds).

CRediT authorship contribution statement

BARRE Abel : Investigation, formal analysis, writing - original draft, writing - review & editing

BRIAND Jean-François : Investigation, methodology, supervision, conceptualization, funding acquisition, project administration, writing - review & editing

VACHER Vincent : Investigation, formal analysis, writing - review & editing

BRIANT Nicolas : Investigation, formal analysis, writing - review & editing

BRIAND Marine : Resources, methodology

DORMOY Bruno : Resources

BOISSERY Pierre : Conceptualization

BOUCHOUCHA Marc : Investigation, conceptualization, supervision, funding acquisition, project administration, writing - review & editing

Declaration of competing interest

The authors declare that they have no known competing financial interests or personal relationships that could have appeared to influence the work reported in this paper.

Acknowledgements

The authors wish to thank all partners involved in the 2021 SUCHIMED campaign (Bouchoucha 2021, SUCHI Med 202 cruise, RV L'Europe, doi:10.17600/18001619), and especially divers C. Ravel, B de Vogue, O. Dugornay, and J.-L. Gonzalez. We thank the anonymous reviewers for their insight and thoughts to improve this manuscript.

Funding

This work was supported by the French Rhone-Mediterranean-Corsica Water Agency through the funding of the BIOFINDIC project (2021-2024).

References

Abdel-Shafy, H.I. and Mansour, M.S.M. (2016) 'A review on polycyclic aromatic hydrocarbons: Source, environmental impact, effect on human health and remediation', *Egyptian Journal of Petroleum*, 25(1), pp. 107–123. Available at: https://doi.org/10.1016/j.ejpe.2015.03.011.

Alter, S.E. *et al.* (2020) 'Evolutionary responses of marine organisms to urbanized seascapes', *Evolutionary Applications*, 14(1), pp. 210–232. Available at: https://doi.org/10.1111/eva.13048.

Andral, B. *et al.* (2004) 'Monitoring chemical contamination levels in the Mediterranean based on the use of mussel caging', *Marine Pollution Bulletin*, 49(9), pp. 704–712. Available at: https://doi.org/10.1016/j.marpolbul.2004.05.008.

Araújo, D.F. *et al.* (2019) 'Copper, zinc and lead isotope signatures of sediments from a mediterranean coastal bay impacted by naval activities and urban sources', *Applied Geochemistry*, 111, p. 104440. Available at: https://doi.org/10.1016/j.apgeochem.2019.104440.

Ayata, S.-D. *et al.* (2018) 'Regionalisation of the Mediterranean basin, a MERMEX synthesis', *Progress in Oceanography*, 163, pp. 7–20. Available at: https://doi.org/10.1016/j.pocean.2017.09.016.

Barral-Fraga, L. *et al.* (2016) 'Short-term arsenic exposure reduces diatom cell size in biofilm communities', *Environmental Science and Pollution Research International*, 23(5), pp. 4257–4270. Available at: https://doi.org/10.1007/s11356-015-4894-8.

Blanco, Y. *et al.* (2018) 'Environmental parameters, and not phylogeny, determine the composition of extracellular polymeric substances in microbial mats from extreme environments', *Science of The Total Environment*, 650. Available at: https://doi.org/10.1016/j.scitotenv.2018.08.440.

Bonnineau, C. *et al.* (2021) 'Role of Biofilms in Contaminant Bioaccumulation and Trophic Transfer in Aquatic Ecosystems: Current State of Knowledge and Future Challenges', in P. de Voogt (ed.) *Reviews of Environmental Contamination and Toxicology Volume 253*. Cham: Springer International Publishing (Reviews of Environmental Contamination and Toxicology), pp. 115–153. Available at: https://doi.org/10.1007/398_2019_39.

Bouchoucha, M. *et al.* (2018) 'Growth, condition and metal concentration in juveniles of two *Diplodus* species in ports', *Marine Pollution Bulletin*, 126, pp. 31–42. Available at: https://doi.org/10.1016/j.marpolbul.2017.10.086.

Briand, J.-F. *et al.* (2017) 'Spatio-Temporal Variations of Marine Biofilm Communities Colonizing Artificial Substrata Including Antifouling Coatings in Contrasted French Coastal Environments', *Microbial Ecology*, 74(3), pp. 585–598. Available at: https://doi.org/10.1007/s00248-017-0966-2.

Briand, J.-F. *et al.* (2022) 'Surface Characteristics Together With Environmental Conditions Shape Marine Biofilm Dynamics in Coastal NW Mediterranean Locations', *Frontiers in Marine Science*, 8. Available at: https://doi.org/10.3389/fmars.2021.746383.

Briand, M.J. *et al.* (2023) 'The French Mussel Watch: More than two decades of chemical contamination survey in Mediterranean coastal waters', *Marine Pollution Bulletin*, 191, p. 114901. Available at: https://doi.org/10.1016/j.marpolbul.2023.114901.

Briant, N. *et al.* (2022) 'Cu isotope records of Cu-based antifouling paints in sediment core profiles from the largest European Marina, The Port Camargue', *Science of The Total Environment*, 849, p. 157885. Available at: https://doi.org/10.1016/j.scitotenv.2022.157885.

Brouwer, A. *et al.* (1999) 'Characterization of potential endocrine-related health effects at low-dose levels of exposure to PCBs.', *Environmental Health Perspectives*, 107(Suppl 4), pp. 639–649.

Cantillo, A.Y. (1998) 'Comparison of results of Mussel Watch Programs of the United States and France with Worldwide Mussel Watch Studies', *Marine Pollution Bulletin*, 36(9), pp. 712–717. Available at: https://doi.org/10.1016/S0025-326X(98)00049-6.

Dang, H. and Lovell, C.R. (2016) 'Microbial Surface Colonization and Biofilm Development in Marine Environments', *Microbiology and Molecular Biology Reviews*, 80(1), pp. 91–138. Available at: https://doi.org/10.1128/MMBR.00037-15.

Derolez, V. *et al.* (2020) 'Two decades of oligotrophication: Evidence for a phytoplankton community shift in the coastal lagoon of Thau (Mediterranean Sea, France)', *Estuarine, Coastal and Shelf Science*, 241, p. 106810. Available at: https://doi.org/10.1016/j.ecss.2020.106810.

Desrosiers, C. *et al.* (2013) 'Bioindicators in marine waters: Benthic diatoms as a tool to assess water quality from eutrophic to oligotrophic coastal ecosystems', *Ecological Indicators*, 32, pp. 25–34. Available at: https://doi.org/10.1016/j.ecolind.2013.02.021.

Djaoudi, K. *et al.* (2022) 'Seawater copper content controls biofilm bioaccumulation and microbial community on microplastics', *Science of The Total Environment*, 814, p. 152278. Available at: https://doi.org/10.1016/j.scitotenv.2021.152278.

Doney, S.C. (2010) 'The Growing Human Footprint on Coastal and Open-Ocean Biogeochemistry', *Science*, 328(5985), pp. 1512–1516. Available at: https://doi.org/10.1126/science.1185198.

Dsikowitzky, L. and Schwarzbauer, J. (2014) 'Organic contaminants from industrial wastewaters: Their identification, toxicity and fate in the environment', *Environ. Chem. Lett.*, 4, pp. 45–101. Available at: https://doi.org/10.1007/978-3-319-02387-8_2.

Fernandes, G. *et al.* (2020) 'The use of epilithic biofilms as bioaccumulators of pesticides and pharmaceuticals in aquatic environments', *Ecotoxicology*, 29(9), pp. 1293–1305. Available at: https://doi.org/10.1007/s10646-020-02259-4.

Flemming, H.-C. and Wingender, J. (2010) 'The biofilm matrix', *Nature Reviews Microbiology*, 8(9), pp. 623–633. Available at: https://doi.org/10.1038/nrmicro2415.

Guigue, C. *et al.* (2023) 'Hydrocarbons in size-fractionated plankton of the Mediterranean Sea (MERITE-HIPPOCAMPE campaign)', *Marine Pollution Bulletin*, 194, p. 115386. Available at: https://doi.org/10.1016/j.marpolbul.2023.115386.

Halpern, B.S. *et al.* (2008) 'A Global Map of Human Impact on Marine Ecosystems', *Science*, 319(5865), pp. 948–952. Available at: https://doi.org/10.1126/science.1149345.

Hobbs, W.O. *et al.* (2019) 'Toxic Burdens of Freshwater Biofilms and Use as a Source Tracking Tool in Rivers and Streams', *Environmental Science & Technology*, 53(19), pp. 11102–11111. Available at: https://doi.org/10.1021/acs.est.9b02865.

Inglis, G.J. and Kross, J.E. (2000) 'Evidence for Systemic Changes in the Benthic Fauna of Tropical Estuaries as a Result of Urbanization', *Marine Pollution Bulletin*, 41(7), pp. 367–376. Available at: https://doi.org/10.1016/S0025-326X(00)00093-X.

Kraak, M.H. *et al.* (1992) 'Chronic ecotoxicity of copper and cadmium to the zebra mussel Dreissena polymorpha', *Archives of Environmental Contamination and Toxicology*, 23(3), pp. 363–369. Available at: https://doi.org/10.1007/BF00216246.

Kriwy, P. and Uthicke, S. (2011) 'Microbial diversity in marine biofilms along a water quality gradient on the Great Barrier Reef', *Systematic and Applied Microbiology*, 34(2), pp. 116–126. Available at: https://doi.org/10.1016/j.syapm.2011.01.003.

Laderriere, V. *et al.* (2022) 'Vulnerability and tolerance to nickel of periphytic biofilm harvested in summer and winter', *Environmental Pollution*, 315, p. 120223. Available at: https://doi.org/10.1016/j.envpol.2022.120223.

Legendre, P. and Legendre, L. (1998) *Numerical ecology. 2nd English Edition, Elsevier, Amsterdam.*

Lenoble, V. *et al.* (2024) 'Bioaccumulation of trace metals in the plastisphere: Awareness of environmental risk from a European perspective', *Environmental Pollution*, 348, p. 123808. Available at: https://doi.org/10.1016/j.envpol.2024.123808.

Lin, H. *et al.* (2020) 'A subcellular level study of copper speciation reveals the synergistic mechanism of microbial cells and EPS involved in copper binding in bacterial biofilms', *Environmental Pollution*, 263, p. 114485. Available at: https://doi.org/10.1016/j.envpol.2020.114485.

Mantel, N. (1967) 'The Detection of Disease Clustering and a Generalized Regression Approach', *Cancer Research*, 27(2_Part_1), pp. 209–220.

Momota, K. and Hosokawa, S. (2021) 'Potential impacts of marine urbanization on benthic macrofaunal diversity', *Scientific Reports*, 11(1), p. 4028. Available at: https://doi.org/10.1038/s41598-021-83597-z.

Oberbeckmann, S. *et al.* (2014) 'Spatial and seasonal variation in diversity and structure of microbial biofilms on marine plastics in Northern European waters', *FEMS Microbiology Ecology*, 90(2), pp. 478–492. Available at: https://doi.org/10.1111/1574-6941.12409.

Oberbeckmann, S., Osborn, A.M. and Duhaime, M.B. (2016) 'Microbes on a Bottle: Substrate, Season and Geography Influence Community Composition of Microbes Colonizing Marine Plastic Debris', *PLOS ONE*. Edited by D.A. Carter, 11(8), p. e0159289. Available at: https://doi.org/10.1371/journal.pone.0159289.

Patel, A.B. *et al.* (2020) 'Polycyclic Aromatic Hydrocarbons: Sources, Toxicity, and Remediation Approaches', *Frontiers in Microbiology*, 11. Available at: https://www.frontiersin.org/articles/10.3389/fmicb.2020.562813 (Accessed: 3 October 2023).

Pesce, S. *et al.* (2024) 'The use of copper as plant protection product contributes to environmental contamination and resulting impacts on terrestrial and aquatic biodiversity and ecosystem functions', *Environmental science and pollution research international* [Preprint]. Available at: https://doi.org/10.1007/s11356-024-32145-z.

Pinto, M. *et al.* (2019) 'The composition of bacterial communities associated with plastic biofilms differs between different polymers and stages of biofilm succession', *PLOS ONE*, 14(6), p. e0217165. Available at: https://doi.org/10.1371/journal.pone.0217165.

Richard, H. *et al.* (2019) 'Biofilm facilitates metal accumulation onto microplastics in estuarine waters', *Science of The Total Environment*, 683, pp. 600–608. Available at: https://doi.org/10.1016/j.scitotenv.2019.04.331.

Rochman, C.M., Hentschel, B.T. and Teh, S.J. (2014) 'Long-Term Sorption of Metals Is Similar among Plastic Types: Implications for Plastic Debris in Aquatic Environments', *PLOS ONE*, 9(1), p. e85433. Available at: https://doi.org/10.1371/journal.pone.0085433.

Sarà, G. *et al.* (1998) 'The relationship between food availability and growth in *Mytilus galloprovincialis* in the open sea (southern Mediterranean)', *Aquaculture*, 167(1), pp. 1–15. Available at: https://doi.org/10.1016/S0044-8486(98)00281-6.

Seed, R. and Suchanek, T.H. (1992) *Seed, R. and Suchanek, T.H. (1992) Population and Community Ecology of Mytilus. In Gosling, E., Ed., The Mussel Mytilus Ecology, Physiology, Genetics and Culture, Elsevier, London, 87-169. - References - Scientific Research Publishing*. Available at: https://www.scirp.org/reference/referencespapers?referenceid=1139224 (Accessed: 3 June 2024).

Soto, D.X. *et al.* (2011) 'Differential accumulation of mercury and other trace metals in the food web components of a reservoir impacted by a chlor-alkali plant (Flix, Ebro River, Spain): Implications for biomonitoring', *Environmental Pollution*, 159(6), pp. 1481–1489. Available at: https://doi.org/10.1016/j.envpol.2011.03.017.

Spalding, M.D. *et al.* (2007) 'Marine Ecoregions of the World: A Bioregionalization of Coastal and Shelf Areas', *BioScience*, 57(7), pp. 573–583. Available at: https://doi.org/10.1641/B570707.

Tan, Karsoon *et al.* (2023) 'Ecological impact of invasive species and pathogens introduced through bivalve aquaculture', *Estuarine, Coastal and Shelf Science*, 294, p. 108541. Available at: https://doi.org/10.1016/j.ecss.2023.108541.

Tessier, E. *et al.* (2011) 'Study of the spatial and historical distribution of sediment inorganic contamination in the Toulon bay (France)', *Marine Pollution Bulletin*, 62(10), pp. 2075–2086. Available at: https://doi.org/10.1016/j.marpolbul.2011.07.022.

582 Tiano, M. *et al.* (2014) 'PCB concentrations in plankton size classes, a temporal study in Marseille Bay,
583 Western Mediterranean Sea', *Marine Pollution Bulletin*, 89(1), pp. 331–339. Available at:
584 https://doi.org/10.1016/j.marpolbul.2014.09.040.

585 Tlili, A. *et al.* (2008) 'Responses of chronically contaminated biofilms to short pulses of diuron: An
586 experimental study simulating flooding events in a small river', *Aquatic Toxicology*, 87(4), pp. 252–263.
587 Available at: https://doi.org/10.1016/j.aquatox.2008.02.004.

588 Tudi, M. *et al.* (2021) 'Agriculture Development, Pesticide Application and Its Impact on the Environment',
589 *International Journal of Environmental Research and Public Health*, 18(3), p. 1112. Available at:
590 https://doi.org/10.3390/ijerph18031112.

591 Wang, Xiufeng *et al.* (2024) 'The extracellular polymeric substances (EPS) accumulation of *Spirulina*
592 *platensis* responding to Cadmium (Cd2+) exposure', *Journal of Hazardous Materials*, 470, p. 134244.
593 Available at: https://doi.org/10.1016/j.jhazmat.2024.134244.

594 Wang, Y. *et al.* (2020) 'Biofilm alters tetracycline and copper adsorption behaviors onto polyethylene
595 microplastics', *Chemical Engineering Journal*, 392, p. 123808. Available at:
596 https://doi.org/10.1016/j.cej.2019.123808.

597 Wolfaardt, G.M. *et al.* (1994) 'Microbial exopolymers provide a mechanism for bioaccumulation of
598 contaminants', *Microbial Ecology*, 27(3), pp. 279–291. Available at: https://doi.org/10.1007/BF00182411.

599 Wolfaardt, G.M. *et al.* (1998) 'In situ Characterization of Biofilm Exopolymers Involved in the Accumulation
600 of Chlorinated Organics', *Microbial Ecology*, 35(3), pp. 213–223. Available at:
601 https://doi.org/10.1007/s002489900077.

602 Zhang, H.-Y. *et al.* (2022) 'Influence of biofilms on the adsorption behavior of nine organic emerging
603 contaminants on microplastics in field-laboratory exposure experiments', *Journal of Hazardous Materials*,
604 434, p. 128895. Available at: https://doi.org/10.1016/j.jhazmat.2022.128895.